Macromolecules

ARTICLE

pubs.acs.org/Macromolecules

# Efficient Low-Temperature Atom Transfer Radical Coupling and Its Application to Synthesis of Well-Defined Symmetrical Polybenzamides

Chih-Feng Huang, Yoshihiro Ohta, Akihiro Yokoyama, and Tsutomu Yokozawa*

Department of Material and Life Chemistry, Kanagawa University, Rokkakubashi, Kanagawa-ku, Yokohama 221-8686, Japan

Supporting Information

**ABSTRACT:** Radical coupling reactions have been widely used for preparation of symmetrical macromolecules. In previous studies of atom transfer radical coupling (ATRC), coupling efficiency above 90% has been generally attained at high temperature ($T$ = 70−110 °C) by using $M_n$ < 5000 precursors. From the mechanistic viewpoint, we designed a strategy for styrene-assisted ATRC from methacrylic macroradicals at low temperature (St/PMMA−Br/Cu$^I$Br/Cu$^0$/Me$_6$TREN). Analysis of the products ($^1$H NMR, H−H COSY, MALDI−TOF mass spectra and gel permeation chromatography) indicated that this provides an efficient "convergent" or coupling approach, if a high degree of chain-end functionality is preserved. We then applied this concept in combination with chain-growth condensation polymerization (CGCP), which usually affords quantitative chain-end functionality. Couplings of high-molecular-weight AB-type diblock polybenzamide, 2-bromoisobutyryl-terminated poly(*N*-octyloxybenzyl-*m*-benzamide)-*block*-poly(*N*-octyl-*m*-benzamide) ($M_n$ = 9300, $M_w/M_n$ = 1.09), were conducted to yield ABA-type triblock polybenzamides with high coupling efficiency (>94%). The molecular weight ($M_n$ ∼ 18000) was doubled and a narrow molecular weight distribution ($M_w/M_n$ < 1.18) was maintained. Selective removal of the octyloxybenzyl groups was achieved, resulting in a poly(*N*-H-*m*-benzamide) segment (i.e., A block). Thermal transitions of the diblock and triblock polybenzamides were examined by DSC. In the case of triblock polybenzamides, the $T_g$ value shifted from 45 to 62 °C after removal of the octyloxybenzyl groups; this might be ascribed to a confinement effect of the segments at the extremities via strong intermolecular hydrogen-bonding interaction.

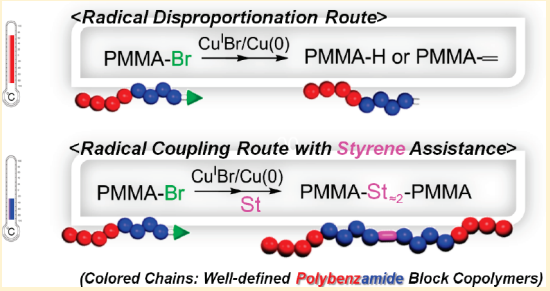


## INTRODUCTION

The discovery in recent decades of controlled/living polymerizations, such as controlled radical polymerizations (CRPs),[1] and ring-opening (metathesis) polymerizations (RO(M)Ps),[2,3] has enabled the design and synthesis of new polymeric materials with unique properties and novel applications. In particular, atom transfer radical polymerization (ATRP) has been proven to be one of the most powerful tools to synthesize well-defined macromolecules. ATRP is generally based on metal-mediated reversible activation/deactivation reactions to prevent recombination and disproportionation of the highly active propagating radicals. The idea of utilizing two radical couplings was developed by Fukuda et al.,[4] and the term "atom transfer radical coupling" (ATRC) was proposed by Yagci,[5] who was the first to demonstrate the synthetic potential of ATRC for the preparation of α,ω-telechelic polystyrene.

In ATRC (Scheme 1), the reaction equilibrium is significantly shifted to the formation of macroradicals by the use of a reducing agent (e.g., nanosize copper, zerovalent iron, tin octanoate, and ascorbic acid) which reduces Cu(II) to Cu(I) species. A high concentration of macroradicals is generated, leading to irreversible termination reactions by coupling. This coupling or "convergent" approach has provided access to telechelic polymers,[6] poly(fluoro)acrylates,[7] ABA triblock copolymers,[8] and H-shaped ABCAB terpolymers.[9] In order to efficiently activate the terminal ATRP initiation site of halopropionates or benzylic halides, the reactions have generally been conducted at high temperature ($T$ = 70−110 °C). However, we considered that side reactions, such

**Scheme 1. General Reaction Mechanism of Cu-Mediated Atom Transfer Radical Coupling (ATRC) (X is a halide atom, $P_n$ is a polymer, and L is a ligand)**

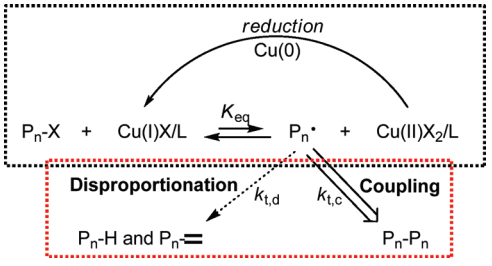


**Received:** March 4, 2011
**Revised:** April 20, 2011
**Published:** May 12, 2011

ACS Publications © 2011 American Chemical Society

as elimination and transfer,[10] might limit the coupling efficiency at high temperature.

A new cobalt-mediated radical coupling (CMRC) method that relies on insertion of diene compounds between the polymer precursors at low temperature was recently developed.[11] With this method, the coupling efficiency is higher than 95% even for high-molecular-weight precursors ($M_n$ = 25000), and a narrow molecular weight distribution is maintained ($M_w/M_n$ = 1.04). Debuigne et al. have reported a practical radical coupling method for (co)polymers by using cobalt-mediated radical polymerization (CMRP).[3]

However, considering that ATRP with a versatile copper catalyst has been used much more widely than CMRP with a cobalt catalyst, it is still of interest to improve the coupling efficiency of ATRC. Previous studies have mainly focused on the coupling of polystyrene (PSt) and poly(methyl acrylate) (PMA) precursors at high temperature. On the other hand, ATRC of poly(methyl methacrylate) (PMMA) precursor could offer the advantage of efficient low-temperature activation. Nevertheless, the PMMA radical is liable to undergo disproportionation rather than coupling, and the value of this strategy remains uncertain.[12,13] But, if styrene were present during ATRC of PMMA precursors, the situation would be drastically changed. The generated PMMA radicals would rapidly cross-propagate to styrene. The formed styryl radicals would undergo not chain extension of the styrene unit at low temperature, but coupling of the polymer. Therefore, ATRC of PMMA precursors, bromo-terminated PMMA (PMMA−Br), should proceed with high efficiency at low temperature in the presence of styrene.

Furthermore, this styrene-assisted ATRC should be applicable to coupling of polymers other than PMMA, because the bromoisobutyrate unit, the radical-generating moiety of PMMA−Br, can easily be introduced into hydroxy-terminal polymers with 2-bromoisobutyryl bromide. We are especially interested in coupling of aromatic polyamides. Owing to their favorable thermal and mechanical properties, aromatic polyamides are considered to be excellent high-performance organic materials (e.g., Fiber, Kevlar, Nomex, and Technora).[14] Recently, there has been great interest in utilizing helical structures[15] and $\beta$-sheet mimicking[16] of polybenzamides to obtain self-assembled nanostructures in solution and in the solid state. We have developed chain-growth condensation polymerization (CGCP) to prepare well-defined block/star polybenzamides through manipulating resonance and inductive effects in monomers.[17] In CGCP, selective activation of the propagating terminal suppresses the reaction of monomers with each other, resulting in controlled molecular weight, low polydispersity, and functionality. Moreover, the well-defined condensation polymers yield telechelic structures that can be utilized or further modified. We have already synthesized hydroxy-terminal polybenzamides, which can be modified to macro chain transfer agents for reversible addition−fragmentation chain transfer (RAFT) polymerization[18] and for use as ATRP macroinitiators.[19] Accordingly, polybenzamides synthesized by CGCP should be useful for styrene-assisted ATRC. Furthermore, poly(*N*-H-benzamide)-*b*-poly(*N*-alkyl-benzamide) diblock copolymer, which affords intriguing self-assembled structures, would be easily convertible to poly(*N*-H-benzamide)-*b*-poly(*N*-alkyl-benzamide)-*b*-poly(*N*-H-benzamide) triblock copolymer by means of this styrene-assisted ATRC.

Here, we first examine styrene-assisted ATRC of PMMA−Br precursors on the basis of previously reported kinetic results. We then present a new approach based on combination of St-assisted ATRC and CGCP for the synthesis of symmetrical ABA-type triblock polybenzamides.

## EXPERIMENTAL SECTION

Details of materials and analyses are provided in the Supporting Information.

**General Procedure for ATRP of MMA.** In a typical experiment, ethyl 2-bromoisobutyrate (EBiB) (68 $\mu$L, 0.47 mmol), MMA (5 mL, 46.7 mmol), *N*,*N*,*N*′,*N*″,*N*‴-pentamethyldiethylenetriamine (PMDETA) (49 $\mu$L, 0.23 mmol), and anisole (5 mL) were charged into a Schlenk flask. The mixture was deoxygenated by means of three freeze−pump−thaw cycles and the flask was backfilled with nitrogen. Then CuBr (23 mg, 0.16 mmol) and $CuBr_2$ (16 mg, 0.07 mmol) were added to the frozen solution. The flask was closed, evacuated and deoxygenated by means of additional two freeze−pump−thaw cycles. An initial sample was taken via a syringe and the flask was then immersed in an oil bath preheated at 40 °C to start the polymerization. The polymerization was stopped at the desired time by placing the flask in an ice bath, and exposing the contents to air. The resulting mixture was diluted with THF and passed through a neutral aluminum oxide column to remove the copper catalyst. The mixture was precipitated in methanol/water =8/2 (v/v). The precipitate was collected by filtration and dried in a vacuum ($M_n$ = 4650, $M_w/M_n$ = 1.38, conversion = 48%, chain-end functionality ($\alpha$) = 0.81 measured by $^1$H NMR).

**CGCP for the Synthesis of Polybenzamide from Initiator 1 and Modifications to 2-Bromoiosbutyryl-Terminated *para*-Type Polybenzamide (PA).** A 10 mL flask equipped with a three-way stopcock was charged with 1.0 M lithium hexamethyldisilazide (LiHMDS)/THF solution (5 mL, 5 mmol). Into the flask was added a mixture of monomer **2** (1.32 g, 5 mmol) and initiator **1** (0.14 g, 0.5 mmol) in dry THF (10 mL) under nitrogen at −10 °C (structures of **1** and **2** are shown in Scheme 4). After the reaction had finished, the mixture was quenched with saturated $NH_4Cl$. The whole was extracted with $CH_2Cl_2$ and the organic layer was washed with water, then dried over $MgSO_4$. The resulting crude oil was dissolved in $CH_2Cl_2$ and twice precipitated into methanol/water =9/1 (v/v) to afford yellowish viscous poly(*N*-octyl-*p*-benzamide) with *tert*-butyldimethylsilyl (TBS) protecting end-group ($M_n$ = 3000, $M_w/M_n$ = 1.08, yield 76%, Figure S1 in the Supporting Information shows the GPC trace).

The resulting poly(*N*-octyl-*p*-benzamide)−OTBS (0.51 g, 0.17 mmol) was dissolved in dry THF (3 mL), and 1.0 M tetrabutylammonium fluoride/tetrahydrofuran (1.0 M TBAF/THF) solution (0.20 mL, 0.20 mmol) was added at room temperature under argon. The mixture was kept at room temperature for 2 h. The reaction mixture was quenched with water, and then extracted with $CH_2Cl_2$. The organic layer was washed with water and dried over anhydrous $MgSO_4$. Yellowish viscous hydroxyl-terminated polybenzamide was obtained (0.48 g, yield 94%). The purified poly(*p*-benzamide)−OH (0.48 g, 0.16 mmol) and triethylamine (0.22 mL, 1.6 mmol) were mixed with dry $CH_2Cl_2$ (10 mL) with stirring for 15 min. A solution of 2-bromoisobutyryl bromide (0.20 mL, 1.6 mmol) in dry $CH_2Cl_2$ (5 mL) was then added dropwise to the mixture with stirring at 0 °C, and stirring was continued at room temperature for 23 h under nitrogen. The reaction mixture was quenched with water, and then extracted with $CH_2Cl_2$. The organic layer was washed with saturated $NaHCO_3$ and water, and the solvent was removed. The crude product was dissolved in $CH_2Cl_2$ and twice precipitated into methanol/water =9/1 (v/v) to give 2-bromoisobutyryl-terminated poly(*N*-octyl-*p*-benzamide) as a yellowish viscous oil (PA, 0.40 g, yield 83%). Quantitative data were obtained from the $^1$H NMR spectrum (see the Supporting Information, Figure S2).

**CGCP for the Synthesis of Diblock Polybenzamide and Modifications to 2-Bromoiosbutyryl-Terminated Diblock *meta*-Type Polybenzamide (diPA).** 50 mL flask, equipped with a three-way stopcock, was charged with LiCl (1.166 g, 27.5 mmol) and dried/backfilled with argon. THF (5 mL) and 1.0 M LiHMDS (5.5 mL, 5.5 mmol) were further charged and the flask was kept at 0 °C over 10 min. Initiator **1** (70 mg, 0.25 mmol) in dry THF (0.5 mL) was then added. Monomer **3** (0.694 g, 2.5 mmol) in dry THF (6 mL) was added dropwise for 25 min via a syringe pump under nitrogen. Monomer **4** (0.923 g, 2.5 mmol)

**Scheme 2. Elementary Reactions of Styrene-Assisted Atom Transfer Radical Coupling ($k_{a,MMA}/k_{da,MMA} = K_{MMA}$; $k_{a,St}/k_{da,St} = K_{St}$)**

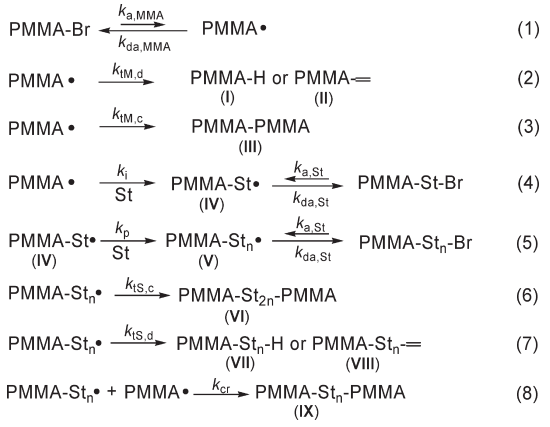


in dry THF (6 mL) was subsequently added dropwise for 20 min under nitrogen (structures of **3** and **4** are shown in Scheme 4). After addition of monomers, the reaction was allowed to continue for 10 min in each case. The reaction was quenched with saturated $NH_4Cl$. The whole was extracted with $CH_2Cl_2$. The combined organic layer was washed with water, and dried over anhydrous $MgSO_4$. Concentration in vacuo gave a crude product as yellow, viscous oil. The oil was dissolved in $CH_2Cl_2$ and twice precipitated into methanol/water = 9/1 (v/v), affording a white-yellow solid after drying ($M_n$ = 9300, $M_w/M_n$ = 1.09, yield 90%; ratio of monomer **3**:**4** = 1.00:1.09 (measured by $^1$H NMR)). The TBS group was removed with 1.0 M TBAF/THF solution. The purified hydroxyl-terminated diblock polybenzamide (yield 78%) was acylated with 2-bromoisobutyryl bromide to obtain 2-bromoisobutyryl-terminated diblock polybenzamide (diPA, yield 84%). Synthetic results for diblock copolymers are given in the Supporting Information, Figures S3−S5.

**General Procedure for ATRC of PMMA−Br, 2-Bromoisobutyryl-Terminated Polybenzamide (PA), and 2-Bromoisobutyryl-Terminated Diblock Polybenzamide (diPA).** An example: the ratio of reagents was St/PA/Cu$^I$Br/Cu$^0$/tris(2-dimethylaminoethyl)amine ($Me_6$TREN) = 40/1/1/4/2.5 in toluene ([PA]$_0$ = 14.5 mM). Styrene, $Me_6$TREN, PA precursor ($M_n$ = 3000), and toluene were added to a 25 mL Schlenk flask. The resulting mixture was deoxygenated by means of three freeze−pump−thaw cycles. The reaction flask was filled with nitrogen, and then Cu$^I$Br and Cu(0) were added to the frozen solution. The flask was closed, evacuated and deoxygenated by means of two additional freeze−pump−thaw cycles. An initial sample was taken via a syringe and the flask was then kept at 25 °C to carry out the coupling reaction. After 5 h, the reaction was stopped by placing the flask in an ice bath, and exposing the contents to air. The resulting mixture was diluted with THF and passed through a neutral aluminum oxide column to remove the copper catalyst. The mixture was twice precipitated into methanol/water =9/1 (v/v). The product was collected by filtration and dried in a vacuum ($M_n$ = 5995, $M_w/M_n$ = 1.08, yield 90%, $x_c \sim 0.99$ calculated from eq 9). Procedures for the removal of the octyloxybenzyl group (OOB) and details of characterization are given in the Supporting Information (Figures S6−S8).

## RESULTS AND DISCUSSION

**Mechanistic Discussion and ATRC of PMMA−Br.** Styrene-assisted atom transfer radical coupling was conducted according to previous fundamental studies. Elementary reactions of radical coupling and reaction rate constants (based on 22 °C) are shown in Scheme 2 and Table 1, respectively. In the absence of styrene, macroradical terminations arise as shown in eqs 1−3 in Scheme 2. It has been reported that termination of methacrylate radical ($k_{t,MMA} \sim 10^8$ L mol$^{-1}$ s$^{-1}$)[20] occurs predominantly by disproportionation.[21,22] Hence, species **I** and **II** are principally obtained, rather than species **III**. Once styrene is introduced, the macroradical termination mechanism is extended as shown in eqs 1−8. There are three key points. First, high ATRP equilibrium constant values ($\sim 10^{-4}$) of both $K_{MMA}$ (eq 1 in Scheme 2 for methyl methacrylate) and $K_{St}$ (eqs 4 and 5 in Scheme 2 for styrene) can provide efficient activation/deactivation reactions, resulting in extension of radical lifetime at low temperature.[23] Second, a very fast addition rate of methacrylic radical to styrene ($k_i \sim 10^3$ L mol$^{-1}$ s$^{-1}$ in eq 4 in Scheme 2) can lead to rapid formation of species **IV**.[24] Third, the St propagation rate constant ($k_p < 10^2$ L mol$^{-1}$ s$^{-1}$) and concentration should be low enough at low temperature so that chain extension is negligible (i.e., $n$ is very small). Owing to the nature of the styrene radical, the

**Table 1. Summary of Reaction Rate Constants for MMA and St[a]**

| constant (22 °C) | value | reference |
|---|---|---|
| $k_{a,MMA}$ (L mol$^{-1}$ s$^{-1}$) | 2.3 × 10$^2$ | 23 |
| $k_{da,MMA}$ (L mol$^{-1}$ s$^{-1}$) | 1.5 × 10$^6$ | 23 |
| $K_{MMA}$ | 1.5 × 10$^{-4}$ | 23 |
| $k_{t,MMA}$ (L mol$^{-1}$ s$^{-1}$) | 6.1 × 10$^8$ | 20 |
| $k_i$ (L mol$^{-1}$ s$^{-1}$) | 5.41 × 10$^3$ | 24 |
| $k_p$ (L mol$^{-1}$ s$^{-1}$) | 86.05 | 23 |
| $k_{a,St}$ (L mol$^{-1}$ s$^{-1}$) | 14 | 23 |
| $k_{da,St}$ (L mol$^{-1}$ s$^{-1}$) | 5.5 × 10$^4$ | 23 |
| $K_{St}$ | 2.6 × 10$^{-4}$ | 23 |
| $k_{t,St}$ (L mol$^{-1}$ s$^{-1}$) | 3.99 × 10$^8$ | 4 |

[a] Key: $k_a$, ATRP activation rate constant; $k_{da}$, ATRP deactivation rate constant; $K$, ATRP equilibrium constant ($=k_a/k_{da}$). These constants were obtained under the conditions described in the references (i.e., values of EBiB for MMA and PEBr for St with CuBr/$Me_6$TREN measured in MeCN at 22 °C). $k_i$, rate constant for addition from methacrylic radical to St (value calculated from the frequency factor and activation energy at 22 °C).[24] $k_p$, propagation rate constant for St. $k_t$, termination rate constant.

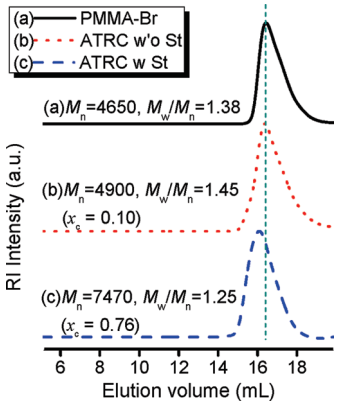


**Figure 1.** GPC traces (RI detector) of (a) PMMA−Br, (b) ATRC of PMMA without St, and (c) ATRC of PMMA with St (St/PMMA−Br/Cu$^I$Br/Cu$^0$/$Me_6$TREN = (0 or 40)/1/1/4/2.5 in toluene at 25 °C; [PMMA−Br]$_0$ = 10.3 mM).

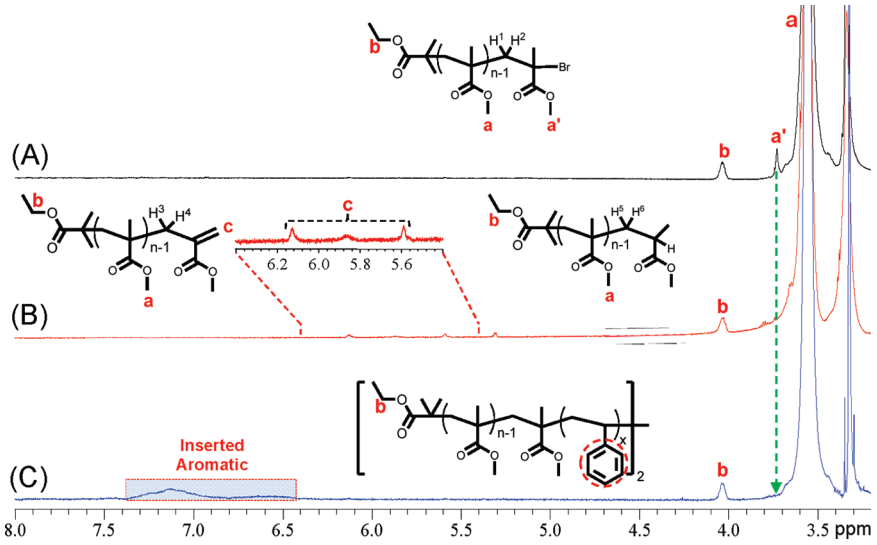


**Figure 2.** $^1$H NMR (600 MHz, DMSO-$d_6$) spectra of (A) PMMA−Br ($M_n$ = 4650, $M_w/M_n$ = 1.38), (B) coupling without St ($M_n$ = 4900, $M_w/M_n$ = 1.45), and (C) coupling with St ($M_n$ = 7470, $M_w/M_n$ = 1.25).

termination ($k_{t,St} \sim 10^8$ L mol$^{-1}$ s$^{-1}$ in eqs 6 and 7 in Scheme 2)[4] is predominantly based on recombination.[4,21,25] Concerning about activity of methacrylic radicals (i.e., fast cross-propagate to styrene and fast self-termination) and steric hindrance, cross-coupling rate ($k_{cr}$) should be slow. Hence, species **VI** is mainly formed rather than species **VII**, **VIII**, and **IX** after termination. Nevertheless, the similar termination rates of methacrylate and styrene radicals would make it challenging to obtain high coupling efficiency.

To examine our hypothesis, ATRC of a monofunctional PMMA−Br precursor ($M_n$ = 4650, $M_w/M_n$ = 1.38), which was obtained by ATRP of MMA, was first carried out (St/PMMA−Br/Cu$^I$Br/Cu$^0$/Me$_6$TREN = (0 or 40)/1/1/4/2.5 in toluene at 25 °C; [PMMA−Br]$_0$ = 10.3 mM). The extent of coupling ($x_c$) was calculated according to eq 9,[6a] where $M_{n,0}$ is the initial number-average molecular weight and $M_n$ is the value after coupling in the absence or presence of styrene:

$$x_c = 2 \times (1 - M_{n,0}/M_n) \quad (9)$$

Figure 1 shows the GPC traces after ATRC of PMMA−Br. As shown in Figure 1b, PMMA ($M_n$ = 4900, $M_w/M_n$ = 1.45) with a low $x_c$ value (0.10) was obtained without styrene, but a small amount of styrene significantly enhanced the coupling reaction, resulting in PMMA ($M_n$ = 7470, $M_w/M_n$ = 1.25) with $x_c$ = 0.76 (Figure 1c).

$^1$H NMR measurements were further conducted. Figure 2 shows the chemical structures and major peak assignments. In Figure 2A, the signal a′ of the chain-end group of PMMA−Br (PMMA-$CH_2C(CH_3)(CO_2CH_3)$−Br: $\delta_{a'}$ = 3.73 ppm) was observed. In ATRC without styrene (Figure 2B), signal c due to the double-bond (PMMA-$CH_2C(CO_2CH_3)$═$CH_2$: $\delta_c$ = 5.59 and 6.13 ppm) was observed, implying that the methacrylic macroradicals underwent disproportionation. From the area of signal c relative to that of signal b, the extent of disproportionation was 0.85. In ATRC in the presence of styrene (Figure 2C), signal a′ also disappeared but disproportionation was suppressed and the signals of inserted St were apparent ($\delta_{aromatic}$ = 7.4−6.4 ppm). From the $^1$H NMR spectrum, the value of inserted St after coupling can be roughly estimated at about 3.50 from the integral areas (i.e., value of $(A_{Ar-H}/5H)/(A_b/4H)$). However, the signals are broad, and there might be inaccuracy, so that the value of inserted St was estimated again by means of MALDI−TOF mass spectrometry (vide infra). In contrast to previous cases (i.e., ATRC at high temperature), these results suggest that activation of the 2-bromoisobutyryl site at low temperature and the presence of styrene in combination afford moderate coupling efficiency. High values of $k_{a,MMA}$ and $k_i$ at low temperature (∼10$^2$ and 10$^3$ listed in Table 1) are, plausibly, responsible for rapid activation of PMMA−Br and fast cross-propagation from the methacrylic macroradicals to styrene, leading to recombination of styryl macroradicals.

H−H COSY measurements were further conducted to acquire detailed information about chain-end variation before and after ATRC in the absence of styrene. For PMMA−Br, the final methylene is adjacent to two chiral carbons at both sides, and two kinds of correlation of the geminal H$^1$ and H$^2$ (labeled in Figure 2A) on the methylene would be observed corresponding to the two chiral carbons (*RR* and *RS*). However, the H−H COSY spectrum of PMMA−Br ($M_n$ = 4650, $M_w/M_n$ = 1.38) relating to the final methylene in the range of 2−3 ppm showed four kinds of correlation with geminal coupling $J_{gem}$ = 13.7 Hz (signals i−k in Figure 3A). This is probably due to the effect of triad chiral centers (*RRR*, *RRS*, *RSR*, *RSS*). Figure 3B shows the H−H COSY spectrum of the resulting polymer ($M_n$ = 4900, $M_w/M_n$ = 1.45) after coupling in the absence of styrene. In this case, the correlation of the methylene signals between 2.45 and 2.65 ppm (H$^3$−H$^6$ labeled in Figure 2B) became narrower but indiscriminable, implying fusion signals of PMMA−H/PMMA-═ via disproportionation. Signal h could be ascribed to a correlation between H$^3$ and H$^4$ based on the *meso* and *racemo* forms of the neighboring diad.[26] Correlated double-bond signals between 6.13 and 5.59 ppm were also observed (see the Supporting Information, Figure S9).

The amount of inserted styrene should be identified to understand the mechanism occurring during the ATRC process. Low-molecular-weight PMMA polymers were analyzed by matrix-assisted laser desorption/ionization time-of-flight mass spectrometry (MALDI−TOF MS) with dithranol as a matrix and potassium trifluoroacetate as a cationizing salt. Figure 4a

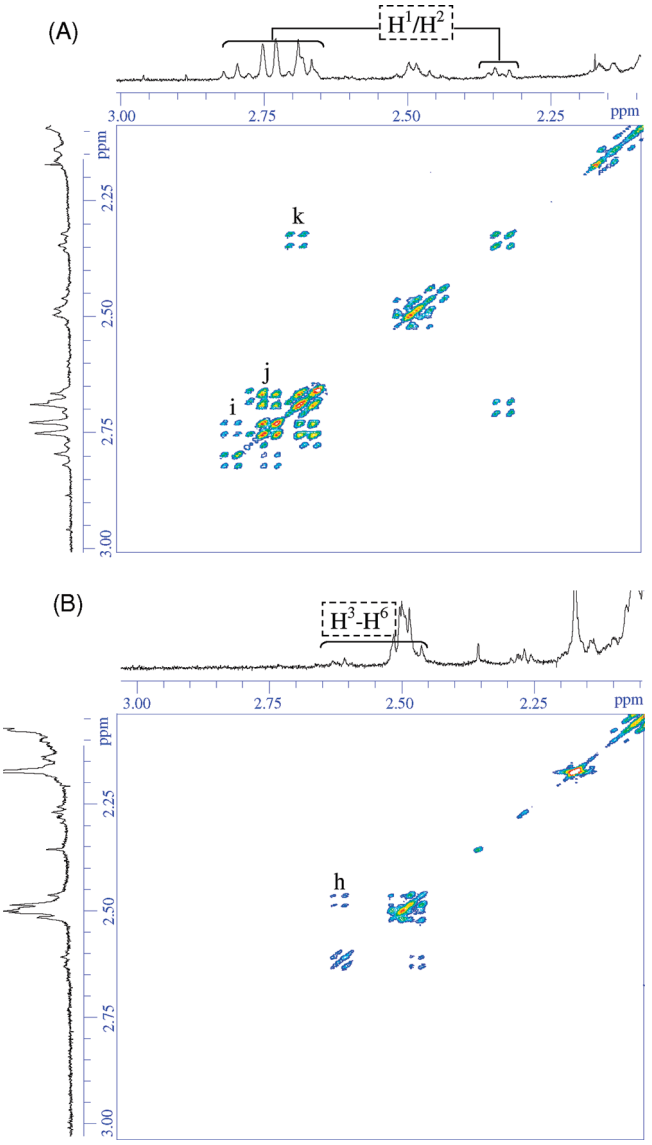


**Figure 3.** H−H COSY (600 MHz, $CDCl_3$) spectra (2−3 ppm) of (A) PMMA−Br ($M_n$ = 4650, $M_w/M_n$ = 1.38) and (B) coupling without St ($M_n$ = 4900, $M_w/M_n$ = 1.45).

illustrates the MALDI−TOF spectrum of PMMA−Br (Scheme 3a: $M_n$ = 1640, $M_w/M_n$ = 1.58), showing a series of peaks separated by approximately 100 Da, which is identical with the molar mass of the repeat unit of PMMA. The enlarged spectrum in Figure 4a ($m/z$ = 1410−1680) shows the peaks with $m/z = MW_{head}(115) + 100m + MW_{end}(1) + K^+$ (39). The bromine of the chain end was lost and hydrogenated (PMMA-H in Scheme 3b). Dehalogenation of PMMA prepared via ATRP is commonly observed during MALDI−TOF measurement, arising from postsource decay of unstable ions that fragment after acceleration in the ion source region.[27] ATRC of this PMMA−Br was then conducted with styrene (St/PMMA−Br/$Cu^IBr/Cu^0$/$Me_6$TREN = 40/1/1/4/2.5 in toluene at 25 °C; $[PMMA-Br]_0$ = 26 mM). Figure 4b shows the MALDI−TOF mass spectrum of the resulting PMMA ($M_n$ = 2680, $M_w/M_n$ = 1.52, $x_c$ = 0.78); two major series of peaks were observed. In the enlarged spectrum, series I (triangles) represents the species resulting from disproportionation of the methacrylic macroradical (i.e., PMMA-H and

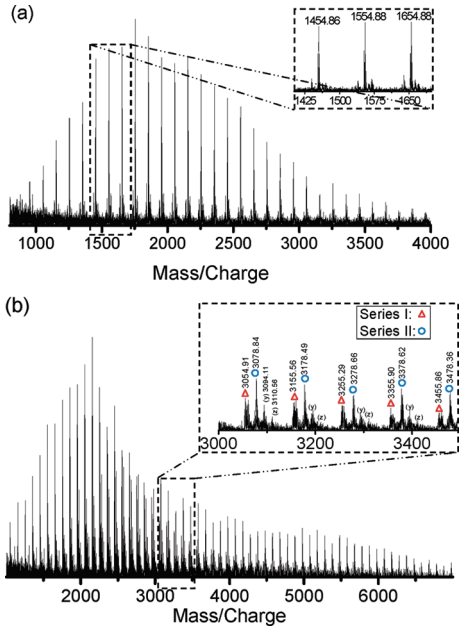


**Figure 4.** MALDI−TOF mass spectra of (a) PMMA−Br ($M_n$ = 1640, $M_w/M_n$ = 1.58) and (b) ATRC of PMMA with St ($M_n$ = 2680, $M_w/M_n$ = 1.52, $x_c$ = 0.78).

**Scheme 3. PMMA Structures with Various Chain-Ends**

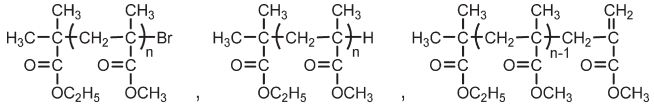


**Table 2. Conditions of Styrene-Assisted Atom Transfer Radical Coupling and Characterization of Products**

| entry[a] | St/PMMA−Br | $T$ (°C) | time (h) | $M_{n,0}$[b] | $M_n$[b] | $x_c$[c] | α[d] | $x_{c,Q}$[e] |
|---|---|---|---|---|---|---|---|---|
| 1 | 0 | 25 | 22 | 4650 | 4900 | 0.10 | 0.81 | 0.12 |
| 2 | 0 | 50 | 22 | 4650 | 5390 | 0.27 | 0.81 | 0.33 |
| 3 | 4 | 25 | 5 | 4650 | 6120 | 0.48 | 0.81 | 0.59 |
| 4 | 4 | 50 | 5 | 4650 | 5740 | 0.38 | 0.81 | 0.47 |
| 5 | 40 | 25 | 18 | 4650 | 7470 | 0.76 | 0.81 | 0.94 |
| 6 | 40 | 50 | 5 | 4650 | 7110 | 0.69 | 0.81 | 0.85 |
| 7 | 0 | 25 | 6 | 1640 | 2090 | 0.43 | 0.79 | 0.54 |
| 8 | 0 | 25 | 4.5 | 2040 | 2490 | 0.36 | 0.68 | 0.53 |
| 9 | 40 | 25 | 5 | 1640 | 2680 | 0.78 | 0.79 | 0.98 |
| 10 | 40 | 25 | 5 | 2040 | 2970 | 0.63 | 0.68 | 0.93 |

[a] St/PMMA−Br/CuBr/$Cu^0$/$Me_6$TREN = $x$/1/1/4/2.5 in toluene; GPC traces (eluent: THF) of entries 1−6 are shown in Figure S10 in the Supporting Information. [b] $M_{n,0}$ and $M_n$ were determined by GPC using poly(methyl methacrylate) calibration standards. [c] $x_c$ (extent of coupling) = $2 \times (1 - M_{n,0}/M_n)$. [d] Chain-end functionality = $(A_a/3)/(A_b/2)$ ($^1$H NMR peak assignments are shown in Figure 2A). [e] $x_{c,Q}$ (deduced extent of coupling with quantitative chain functionality) ≡ $x_c/\alpha$.

PMMA-= in Scheme 3b and 3c). On the other hand, series II (circles) corresponds to PMMA coupling products containing two styrene units (i.e., $m/z = MW_{head+end}(115 \times 2) + 100m +$

**Scheme 4. Synthesis of Well-Defined Symmetrical Polybenzamides by Means of Combination of Styrene-Assisted Atom Transfer Radical Coupling and Chain-Growth Condensation Polymerization**

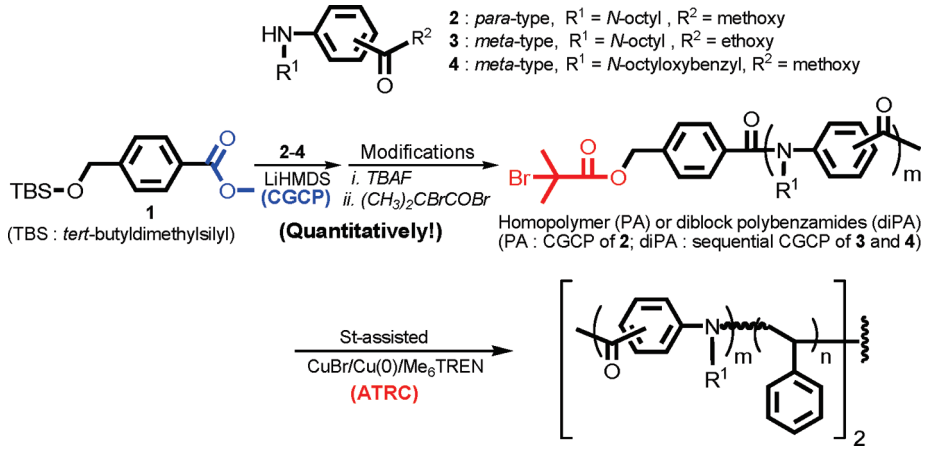


**Scheme 5. Precursors of (a) Polybenzamide Homopolymer (PA) and (b) Diblock Polybenzamide (diPA) for Coupling Reactions**

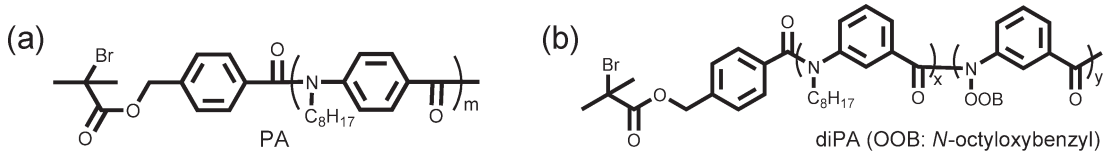


$MW_{styrene} \times n$ (104 × 2) + $K^+$ (39)). We further checked the (*y*) and (*z*) series in the enlarged spectrum; larger amounts of styrene insertions (i.e., $n > 2$) can be neglected. The 2 small series might be due to fragmentations of the coupled PMMA (see the Supporting Information: Table S1 and Scheme S1). The above result strongly supports our hypothesis that the St propagation rate constant ($k_p < 10^2$ L mol$^{-1}$ s$^{-1}$) and concentration are sufficiently low, resulting in only a small amount of St insertion ($n \approx 2$) at room temperature.

On the basis of these observations, the mechanism is proposed to be as follows: (1) generation of PMMA$^\bullet$ radicals from PMMA−Br precursor; (2) addition of a few styrene units leading to PMMA−St$_n^\bullet$ macroradicals ($n \approx 1$); and (3) fast coupling of PMMA−St$_n^\bullet$ macroradical to yield a symmetrical coupling product (PMMA−St$_{\approx 2}$−PMMA), as well as release of $Cu^{II}Br_2$. It is worth mentioning that the deactivation of PMMA−St$_n^\bullet$ macroradical and its reactivation would make a negligible contribution under low-temperature reaction conditions (i.e., $k_{a,St} \ll k_{da,St} \ll k_{t,St}$; see Table 1).

Low-temperature (25 and 50 °C) coupling reactions of PMMA−Br precursors with various amounts of St were conducted. Table 2 summarizes the reaction conditions and results of characterization. The GPC traces of entries 3−6 in Table 2 showed obvious shifts with unimodal molecular weight distributions (see Figure S10 in the Supporting Information). Apparently, the extent of coupling ($x_c$) is significantly enhanced in the presence of an appropriate amount of St (entries 5, 6, 9, and 10 in Table 2): 40 equiv of St to PMMA−Br at 25 °C gave the highest $x_c$ (entries 5 and 9). If the chain-end functionality (α) of PMMA−Br (measured by $^1$H NMR) is considered, the extent of coupling with quantitative chain functionality ($x_{c,Q} \equiv x_c/\alpha$ in Table 2) could be higher than 0.90. Thus, this method could provide an efficient coupling approach if the coupling precursors have a high degree of chain-end functionality.

**Table 3. Conditions of Polybenzamide Homopolymer (PA) Couplings and Characterization of Products**

| entry[a] | St/PA | *T* (°C) | time (h) | $M_{n,0}(M_w/M_n)^b$ | $M_n(M_w/M_n)^b$ | $x_c{}^c$ |
|---|---|---|---|---|---|---|
| 1 | 0 | 25 | 20 | 3000 (1.08) | 3790 (1.08) | 0.40 |
| 2 | 0 | 50 | 17 | 3000 (1.08) | 4070 (1.16) | 0.52 |
| 3 | 0 | 70 | 19 | 3000 (1.08) | 4270 (1.15) | 0.59 |
| 4 | 4 | 25 | 9 | 3000 (1.08) | 5093 (1.13) | 0.81 |
| 5 | 4 | 50 | 17 | 3000 (1.08) | 5200 (1.12) | 0.85 |
| 6 | 4 | 70 | 12 | 3000 (1.08) | 4950 (1.14) | 0.78 |
| 7 | 40 | 25 | 5.5 | 3000 (1.08) | 5995 (1.08) | 0.99 |
| 8 | 40 | 50 | 17 | 3000 (1.08) | 5810 (1.16) | 0.97 |
| 9 | 40 | 70 | 17 | 3000 (1.08) | 4500 (1.12) | 0.66 |
| 10 | 80 | 25 | 19.5 | 3000 (1.08) | 5990 (1.08) | 0.99 |
| 11 | 80 | 50 | 11 | 3000 (1.08) | 6000 (1.08) | 0.99 |
| 12 | 80 | 70 | 10.5 | 3000 (1.08) | 6620 (1.23) | >1[d] |

[a] St/PA/CuBr/Cu$^0$/Me$_6$TREN = *x*/1/1/4/2.5 in toluene. [b] $M_{n,0}$ and $M_n$ were determined by GPC using polystyrene calibration standards. [c] $x_c$ (extent of coupling) = 2 × (1 − $M_{n,0}/M_n$). [d] A large amount of St was incorporated by chain extension from PA macroinitiator.

**Practical Synthesis of Polybenzamide Homo- and Block Copolymers and Thermal Properties.** We have developed chain-growth condensation polymerization (CGCP) to prepare well-defined polybenzamides. The well-defined condensation polymers yield quantitatively telechelic structures. Building on this, our strategy for combination with CGCP (herein,


dx.doi.org/10.1021/ma200494m |*Macromolecules* 2011, 44, 4140–4148

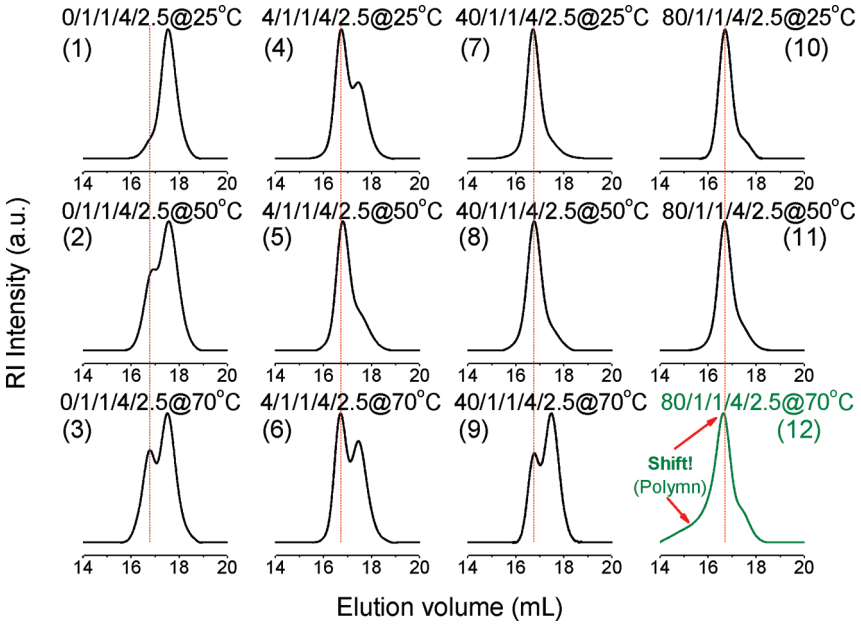


**Figure 5.** GPC traces (RI detector) after ATRC of PA (St/PA/Cu$^{I}$Br/Cu$^{0}$/Me$_6$TREN = $x$/1/1/4/2.5 in toluene; [PA]$_0$ = 14.5 mM).

**Table 4. Conditions of Diblock Polybenzamide (diPA) Couplings and Characterization of Products**

| entry[a] | St/diPA | $T$ (°C) | time (h) | $M_{n,0}$($M_w$/$M_n$)[b] | $M_n$($M_w$/$M_n$)[b] | $x_c$[c] |
|---|---|---|---|---|---|---|
| 1 | 40 | 25 | 21 | 9300 (1.09) | 17500 (1.11) | 0.94 |
| 2 | 40 | 50 | 21 | 9300 (1.09) | 17800 (1.09) | 0.95 |
| 3 | 80 | 25 | 5 | 9300 (1.09) | 17500 (1.10) | 0.94 |
| 4 | 80 | 50 | 19 | 9300 (1.09) | 17940 (1.17) | 0.96 |

[a] St/diPA/CuBr/Cu$^0$/Me$_6$TREN = $x$/1/1/4/2.5 in toluene. [b] $M_{n,0}$ and $M_n$ were determined by GPC using polystyrene calibration standards. [c] $x_c$ (the extent of coupling) = 2 × (1 − $M_{n,0}$/$M_n$).

polybenzamides) and St-assisted ATRC is illustrated in Scheme 4. Two 2-bromoisobutyryl-terminated polybenzamide precursors (shown in Scheme 5), poly(*N*-octyl-*p*-benzamide) (PA: $M_n$ = 3000, $M_w$/$M_n$ = 1.08) and poly(*N*-octyl-*m*-benzamide)-*block*-poly(*N*-octyloxybenzyl-*m*-benzamide) (diPA: $M_n$ = 9300, $M_w$/$M_n$ = 1.09), were prepared.

Coupling reactions of PA (Scheme 5a) were examined systematically (Table 3). Figure 5 shows the GPC traces of the resulting coupling products, in which two distinct peaks can be seen (at elution times of ~16.7 and 17.7 min). Without St (entries 1−3 in Table 3), $x_c$ increased with temperature, but remained low (<0.59). At low temperature, $x_c$ increased with increasing amount of St, and high coupling efficiencies (>0.97) were obtained at St/PA ratios above 40 (entries 7, 8, 10, and 11). At 25 °C, the coupling reaction was completed ($x_c$ ~ 0.99) in 3 h (see the Supporting Information Figures S11 and S12), implying that the coupling reaction was fast. After coupling of PA, the amount of inserted styrene units ($n \approx 2$) was also confirmed by MALDI−TOF measurements (see the Supporting Information Figure S13 and Table S2). At 70 °C, the reactions (entries 6 and 9) gave lower $x_c$ values than were obtained at low temperature, possibly due to enhancement of side reactions. When the St/PA ratio was equal to 80, chain extension was observed from the peak shifting, but the molecular weight distribution became broad. Table 3 summarizes

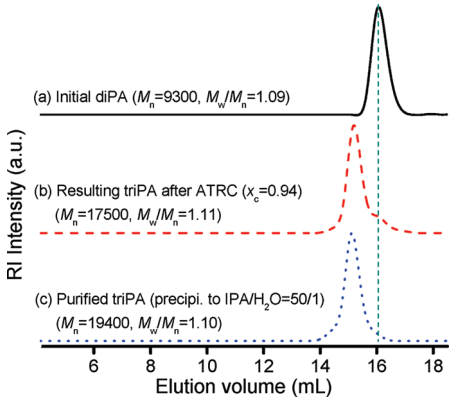


**Figure 6.** GPC traces (RI detector) of diblock polybenzamide coupling products: (a) initial diblock polybenzamide (diPA), (b) crude triblock polybenzamide (triPA) after ATRC, and (c) purified triPA (precipitated into IPA/H$_2$O = 50/1 (v/v)).

the conditions and results of the coupling reactions. In summary, low temperature is essential for the suppression of St propagation and side reaction of macroradicals. An appropriate amount of St is the key to attenuate the self-termination of methacrylic macroradicals and leads to high coupling efficiency.

St-assisted ATRC was further applied to the coupling of well-defined diblock polybenzamide (diPA in Scheme 5b). Table 4 summarizes the conditions and coupling results. High coupling efficiencies were maintained ($x_c$ ~ 0.95), and ABA-type triblock polybenzamides (triPA) were successfully obtained with nearly double the initial molecular weight ($M_n$ ~ 18000), while the molecular weight distribution remained narrow ($M_w$/$M_n$ < 1.18). In previous studies of ATRC, $x_c$ > 0.9 was usually obtained with $M_n$ < 5000 precursors. Herein, coupling of a high-molecular-weight precursor ($M_n$ = 9300) was achieved with high coupling efficiency (>0.94). Further purification was carried out by fractional precipitation into a mixture of isopropyl alcohol and water (volume ratio of

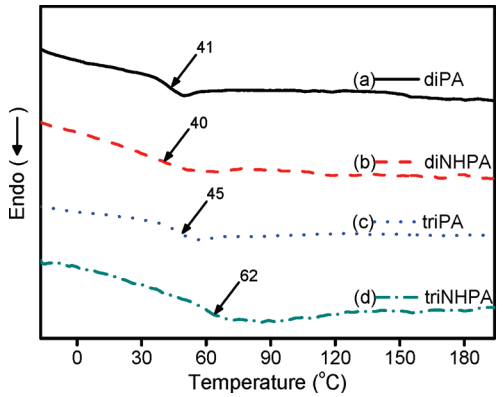


**Figure 7.** DSC traces of polybenzamides before and after deprotection of OOB group: (a) diPA, (b) diNHPA, (c) triPA, and (d) triNHPA (samples were annealed at 150 °C under vacuum for 2 days before measurements).

IPA/$H_2O$ = 50/1). As shown in Figure 6, the small amount of diblock copolymer was effectively removed to yield triblock copolymer ($M_n$ = 19400, $M_w/M_n$ = 1.10, yield 52%) with high purity.

One of the features of polybenzamide is self-assembly via strong intermolecular hydrogen-bonding. Thus, selective removal of the octyloxybenzyl group (OOB) was further conducted with trifluoroacetic acid (TFA) for 3 days to synthesize poly(*N*-H-*m*-benzamide)-*b*-poly(*N*-octyl-*m*-benzamide)-*b*-poly(*N*-H-*m*-benzamide) triblock copolymer (triNHPA: $M_n$ = 15560, $M_w/M_n$ = 1.19). Characterization data (GPC traces and $^1$H NMR and FT-IR spectra) are shown in the Supporting Information (Figures S6−S8). These results indicated that selective deprotection and good stability of the ester linkage were both attained. Thermal transitions of these diblock and triblock polybenzamides were examined by DSC at a heating rate of 10 °C/min under nitrogen (Figure 7). In the case of AB-type diblock copolymers (i.e., curves (a) diPA and (b) diNHPA), nearly unchanged glass transition temperature ($T_g \sim 40$ °C) was observed. In the case of ABA-type triblock copolymers (i.e., curves (c) triPA and (d) triNHPA), however, the $T_g$ value significantly shifted from 45 to 62 °C. This might be because the midchain (i.e., B block) was confined by the chains at the extremities (i.e., the two A blocks) via intermolecular hydrogen-bonding interaction. Investigations of the self-assembly behavior of various polybenzamide-based triblock copolymers in solution and in the solid state are under way.

## CONCLUSIONS

On the basis of mechanistic considerations, we developed a strategy for radical recombination of methacrylic macroradicals with the assistance of styrene. The results of GPC and $^1$H NMR and MALDI−TOF spectra indicated that disproportionation of methacrylic macroradicals occurred predominantly in the absence of styrene. However, in the presence of styrene, ATRC from PMMA−Br precursor proceeded at low temperature, with a moderate extent of coupling ($x_c \sim 0.76$). These results are consistent with the following mechanism: (1) generation of PMMA$^\bullet$ radical from PMMA−Br; (2) addition of a few styrene units to afford PMMA−St$_n^\bullet$ macroradical ($n \sim 1$); and (3) fast coupling of PMMA−St$_n^\bullet$ macroradicals with each other, leading to the formation of the coupling product (PMMA−St$_{\approx 2}$−PMMA). If PMMA−Br has high chain-end functionality, efficient St-assisted ATRC of PMMA−Br can be achieved. We extended this concept to coupling of polybenzamides obtained by CGCP, in which quantitative chain-end functionality is acquired. The St-assisted ATRC of homo ($M_n$ = 3000) and diblock ($M_n$ = 9300) polybenzamides proceeded with a high extent of coupling ($x_c > 0.94$), and the molecular weight nearly doubled ($M_n \sim 6000$ and $M_n \sim 18000$), while a narrow molecular weight distribution was retained ($M_w/M_n < 1.18$). In the case of the polybenzamide block copolymers, selective removal of the OOB group and good stability of the ester linkage resulted in the formation of poly(*N*-H-polybenzamide) segments. Thermal transitions of these diblock and triblock polybenzamides (i.e., diPA, diNHPA, triPA, and triNHPA) were examined by DSC. In the case of triblock polybenzamides, the $T_g$ value significantly shifted from 45 to 62 °C after deprotection, possibly due to a confinement effect of the chains at the extremities via intermolecular hydrogen-bonding. In summary, we have designed a new approach, based on combination of styrene-assisted atom transfer radical coupling and chain-growth condensation polymerization, for the synthesis of symmetrical ABA-type triblock polybenzamides and demonstrated its effectiveness.

## ASSOCIATED CONTENT

**Supporting Information.** Materials and analyses of $^1$H NMR, GPC, FT-IR, and MALDI−TOF data. This material is available free of charge via the Internet at http://pubs.acs.org.

## AUTHOR INFORMATION

### Corresponding Author

*Fax: +81-45-413-9770. E-mail: yokozt01@kanagawa-u.ac.jp.

## ACKNOWLEDGMENT

This study was supported by a Scientific Frontier Research Project Grant from the Ministry of Education, Science, Sport, and Culture, Japan.

## REFERENCES

(1) (a) Coessens, V.; Pintauer, T.; Matyjaszewski, K. *Prog. Polym. Sci.* **2001**, *26*, 337–377. (b) Kamigaito, M.; Ando, T.; Sawamoto, M. *Chem. Rev.* **2001**, *101*, 3689–3745. (c) Hawker, C. J.; Bosman, A. W.; Harth, E. *Chem. Rev.* **2001**, *101*, 3661–3688. (d) Yamago, S.; Kayahara, E.; Kotani, M.; Ray, B.; Kwak, Y.; Goto, A.; Fukuda, T. *Angew. Chem., Int. Ed.* **2007**, *46*, 1304–1306. (e) Moad, G.; Rizzardo, E.; Thang, S. H. *Polymer* **2008**, *49*, 1079–1131. (f) Braunecker, W. A.; Matyjaszewski, K. *Prog. Polym. Sci.* **2007**, *32*, 93–146.

(2) (a) Mecerreyes, D.; Jerome, R.; Dubois, P. *Adv. Polym. Sci.* **1999**, *147*, 1–59. (b) Trnka, T. M.; Grubbs, R. H. *Acc. Chem. Res.* **2001**, *34*, 18–29.

(3) Debuigne, A.; Poli, R.; Jerome, C.; Jerome, R.; Detrembleur, C. *Prog. Polym. Sci.* **2009**, *34*, 211–239.

(4) Yoshikawa, C.; Goto, A.; Fukuda, T. *e-Polym.* **2002**, no. 13.

(5) Yurteri, S.; Cianga, I.; Yagci, Y. *Macromol. Chem. Phys.* **2003**, *204*, 1771–1783.

(6) (a) Sarbu, T.; Lin, K. Y.; Ell, J.; Siegwart, D. J.; Spanswick, J.; Matyjaszewski, K. *Macromolecules* **2004**, *37*, 3120–3127. (b) Nottelet, B.; Lacroix-Desmazes, P.; Boutevin, B. *Polymer* **2007**, *48*, 50–57. (c) Otazaghine, B.; Boyer, C.; Robin, J. J.; Boutevin, B. *J. Polym. Sci., Part A: Polym. Chem.* **2005**, *43*, 2377–2394. (d) Kopping, J. T.; Tolstyka, Z. P.; Maynard, H. D. *Macromolecules* **2007**, *40*, 8593–8599. (e) Otazaghine, B.; David, G.; Boutevin, B.; Robin, J. J.; Matyjaszewski, K. *Macromol. Chem. Phys.* **2004**, *205*, 154–164.

(7) (a) Otazaghine, B.; Boutevin, B. *Macromol. Chem. Phys.* **2004**, *205*, 2002–2011. (b) Sarbu, T.; Lin, K. Y.; Spanswick, J.; Gil, R. R.; Siegwart, D. J.; Matyjaszewski, K. *Macromolecules* **2004**, *37*, 9694–9700.
(8) Nagelsdiek, R.; Keul, H.; Hocker, H. *e-Polym.* **2005**, no. 49.
(9) Luo, X. L.; Wang, G. W.; Huang, J. L. *J. Polym. Sci., Part A: Polym. Chem.* **2009**, *47*, 59–68.
(10) Lutz, J. F.; Matyjaszewski, K. *J. Polym. Sci., Part A: Polym. Chem.* **2005**, *43*, 897–910.
(11) (a) Debuigne, A.; Jerome, C.; Detrembleur, C. *Angew. Chem., Int. Ed.* **2009**, *48*, 1422–1424. (b) Debuigne, A.; Poli, R.; De Winter, J.; Laurent, P.; Gerbaux, P.; Dubois, P.; Wathelet, J. P.; Jerome, C.; Detrembleur, C. *Chem.—Eur. J.* **2010**, *16*, 1799–1811. (c) Debuigne, A.; Poli, R.; De Winter, J.; Laurent, P.; Gerbaux, P.; Wathelet, J. P.; Jerome, C.; Detrembleur, C. *Macromolecules* **2010**, *43*, 2801–2813.
(12) (a) Sasaki, D.; Suzuki, Y.; Hagiwara, T.; Yano, S.; Sawaguchi, T. *Polymer* **2008**, *49*, 4094–4100. (b) Wrue, M. H.; McUmber, A. C.; Anthamatten, M. *Macromolecules* **2009**, *42*, 9255–9262.
(13) Jiang, X. Z.; Vamvakaki, M.; Narain, R. *Macromolecules* **2010**, *43*, 3228–3232.
(14) Garcia, J. M.; Garcia, F. C.; Serna, F.; de la Pena, J. L. *Prog. Polym. Sci.* **2010**, *35*, 623–686.
(15) (a) Yamazaki, K.; Yokoyama, A.; Yokozawa, T. *Macromolecules* **2006**, *39*, 2432–2434. (b) Mikami, K.; Tanatani, A.; Yokoyama, A.; Yokozawa, T. *Macromolecules* **2009**, *42*, 3849–3851. (c) Tanatani, A.; Yokoyama, A.; Azumaya, I.; Takakura, Y.; Mitsui, C.; Shiro, M.; Uchiyama, M.; Muranaka, A.; Kobayashi, N.; Yokozawa, T. *J. Am. Chem. Soc.* **2005**, *127*, 8553–8561.
(16) (a) Seyler, H.; Kilbinger, A. F. M. *Macromolecules* **2009**, *42*, 9141–9146. (b) Konig, H. M.; Kilbinger, A. F. M. *Angew. Chem., Int. Ed.* **2007**, *46*, 8334–8340. (c) Schleuss, T. W.; Abbel, R.; Gross, M.; Schollmeyer, D.; Frey, H.; Maskos, M.; Berger, R.; Kilbinger, A. F. M. *Angew. Chem., Int. Ed.* **2006**, *45*, 2969–2975.
(17) (a) Sugi, R.; Hitaka, Y.; Yokoyama, A.; Yokozawa, T. *Macromolecules* **2005**, *38*, 5526–5531. (b) Sugi, R.; Yokoyama, A.; Furuyama, T.; Uchiyama, M.; Yokozawa, T. *J. Am. Chem. Soc.* **2005**, *127*, 10172–10173. (c) Yokozawa, T.; Ogawa, M.; Sekino, A.; Sugi, R.; Yokoyama, A. *J. Am. Chem. Soc.* **2002**, *124*, 15158–15159. (d) Yokozawa, T.; Yokoyama, A. *Prog. Polym. Sci.* **2007**, *32*, 147–172. (e) Yokozawa, T.; Yokoyama, A. *Chem. Rev.* **2009**, *109*, 5595–5619. (f) Ohishi, T.; Sugi, R.; Yokoyama, A.; Yokozawa, T. *Macromolecules* **2008**, *41*, 9683–9691. (g) Yokozawa, T.; Asai, T.; Sugi, R.; Ishigooka, S.; Hiraoka, S. *J. Am. Chem. Soc.* **2000**, *122*, 8313–8314. (h) Yoshino, K.; Yokoyama, A.; Yokozawa, T. *J. Polym. Sci., Part A: Polym. Chem.* **2009**, *47*, 6328–6332.
(18) Masukawa, T.; Yokoyama, A.; Yokozawa, T. *Macromol. Rapid Commun.* **2009**, *30*, 1413–1418.
(19) Huang, C. F.; Yokoyama, A.; Yokozawa, T. *J. Polym. Sci., Part A: Polym. Chem.* **2010**, *48*, 2948–2954.
(20) Barth, J.; Buback, M. *Macromol. Rapid Commun.* **2009**, *30*, 1805–1811.
(21) Zammit, M. D.; Davis, T. P.; Haddleton, D. M.; Suddaby, K. G. *Macromolecules* **1997**, *30*, 1915–1920.
(22) Bevington, J. C.; Melville, M. H.; Taylor, R. P. *J. Polym. Sci.* **1954**, *14*, 463–476.
(23) (a) Tang, W.; Kwak, Y.; Braunecker, W.; Tsarevsky, N. V.; Coote, M. L.; Matyjaszewski, K. *J. Am. Chem. Soc.* **2008**, *130*, 10702–10713. (b) Tang, W.; Matyjaszewski, K. *Macromol. Theor. Simul.* **2008**, *17*, 359–375. (c) Tang, W.; Tsarevsky, N. V.; Matyjaszewski, K. *J. Am. Chem. Soc.* **2006**, *128*, 1598–1604.
(24) Fischer, H.; Radom, L. *Angew. Chem., Int. Ed.* **2001**, *40*, 1340–1371.
(25) (a) Gleixner, G.; Olaj, O. F.; Breitenbach, J. W. *Makromol. Chem.* **1979**, *180*, 2581–2598. (b) Moad, G.; Solomon, D. H.; Johns, S. R.; Willing, R. I. *Macromolecules* **1984**, *17*, 1094–1099.
(26) Hatada, K.; Kitayama, T.; Ute, K.; Terawaki, Y.; Yanagida, T. *Macromolecules* **1997**, *30*, 6754–6759.
(27) (a) Jackson, A. T.; Bunn, A.; Priestnall, I. M.; Borman, C. D.; Irvine, D. J. *Polymer* **2006**, *47*, 1044–1054. (b) Singha, N. K.; Rimmer, S.; Klumperman, B. *Eur. Polym. J.* **2004**, *40*, 159–163.